



## Archive-Based Ions Motion Optimization for the Multi-Objective Optimal Power Flow Problem and its Techno-Economic-Environmental Benefit Assessment

**Hitarth Buch**

Department of Electrical Engineering, L. E. College, Morbi, Gujarat, India

\* Corresponding Author: **Hitarth Buch**

---

### Article Info

**P-ISSN:** 3051-3383

**E-ISSN:** 3051-3391

**Volume:** 02

**Issue:** 01

**Received:** 22-01-2021

**Accepted:** 10-03-2021

**Published:** 15-04-2021

**Page No:** 49-55

### Abstract

The optimal power flow (OPF) problem is a large-scale, non-linear and non-convex optimization task that underpins the economic and secure operation of modern power systems. When several conflicting goals—fuel cost, active power loss and emission—are pursued simultaneously, no single operating point optimizes all objectives, and a set of trade-off solutions must be produced. This paper applies an archive-based multi-objective Ions Motion Optimization algorithm (MOIMO) to the multi-objective OPF (MOOPF) problem. The single-objective Ions Motion Optimization is extended to many objectives through an external archive that retains the non-dominated solutions found so far and a leader-selection strategy that steers the search toward the least-crowded region of the Pareto front, thereby preserving diversity. MOIMO is benchmarked against six contemporary archive-based optimizers on ten MOOPF cases formulated over the IEEE 30-, 57- and 118-bus systems, with realistic cost models that include valve-point loading, multi-fuel and prohibited operating zones. Performance is judged by the best compromised solution, Pareto-front spread, computation time, hyper-volume and three statistical tests. MOIMO returns uniformly distributed Pareto fronts and the lowest standard deviation of hyper-volume in four of ten cases, confirming its robustness, while statistical tests rank MOMVO first overall, in line with the No Free Lunch theorem. A techno-economic-environmental assessment of the quadratic-fuel-cost-and-emission compromise solution shows an annual fuel saving of 117,988 \$ and an emission reduction of 298.716 tons relative to a reported method, demonstrating the practical value of the approach.

**DOI:** <https://doi.org/10.54660/IJAIET.2021.2.1.49-55>

**Keywords:** Optimal Power Flow, Multi-objective Optimization, Ions Motion Optimization, Pareto front, Hyper-volume, Emission reduction

---

### 1. Introduction

Optimal economic planning and operation of power generation remain central concerns for the electricity industry. When power is delivered from several generating units to meet a continually varying load, each generator output must be set so that the overall fuel cost is held to a minimum while every operating limit is respected. The optimal power flow problem combines the economic dispatch and the power-flow sub-problems into a single optimization task, and it is therefore solved as a routine yet demanding operation in power-system control centres.

Because of the valve-point loading effect, the use of multiple fuels, transformer tap settings and shunt compensation, the OPF is a non-linear, non-convex and non-smooth problem. Classical gradient-based methods require differentiable and continuous objective functions and frequently converge to local optima for such complex formulations. These limitations can be circumvented with derivative-free, population-based metaheuristics, which use only fitness information and follow stochastic rather than deterministic transition rules. A large body of work has consequently applied metaheuristics to the single-objective OPF problem <sup>[1, 2]</sup>.

Practical operation, however, rarely depends on a single objective. Fuel cost, active power loss and emission generally conflict, so no operating point optimizes all of them at once; instead, a family of equally valid trade-off, or Pareto-optimal, solutions exist<sup>[3]</sup>. The multi-objective OPF problem therefore requires algorithms that not only converge toward the true Pareto front but also distribute solutions uniformly across it. The No Free Lunch theorem<sup>[4]</sup> implies that no single multi-objective optimizer dominates on every problem, which keeps the search for effective new approaches open.

This paper extends the Ions Motion Optimization (IMO) algorithm of Javidy *et al.*<sup>[5]</sup> to the multi-objective domain through an external archive and a leader-selection mechanism, producing the archive-based MOIMO, and applies it to the multi-objective OPF problem. The contributions are threefold: (i) an archive-based multi-objective formulation of IMO that maintains diversity through crowding-aware leader selection; (ii) a comprehensive comparison against six contemporary archive-based optimizers on ten MOOPF cases drawn from the IEEE 30-, 57- and 118-bus systems using best compromised solution, hyper-volume and statistical tests; and (iii) a techno-economic-environmental quantification of the resulting compromise solutions, expressed as annual cost, emission and loss savings.

## 2. Multi-Objective OPF Formulation

The MOOPF problem minimizes a vector of objective functions subject to the power-flow equality constraints and the operating inequality constraints. It is stated as

$$\text{Minimize } F(x, u) = [f_1(x, u), f_2(x, u), \dots, f_m(x, u)]$$

subject to  $g(x, u) = 0$  and  $h(x, u) \leq 0$ , where  $x$  is the vector of state (dependent) variables and  $u$  the vector of control (independent) variables. The control variables comprise the generator active powers (except the slack bus), generator bus voltages, transformer tap settings and shunt VAR compensation. The state variables comprise the slack-bus power, load-bus voltages, generator reactive powers and line loadings. The equality constraints  $g$  are the nodal real- and reactive-power balance equations; the inequality constraints  $h$  enforces generator, voltage, tap, compensation and line-flow limits.

### 2.1. Objective Functions

Four classes of objective are considered. The **quadratic fuel cost** (QFC) expresses generation cost as a quadratic function of generator output. The **total fuel cost** (TFC) augments the quadratic model with the valve-point loading effect (a rectified-sinusoid term), multi-fuel options (piecewise-quadratic cost) and prohibited operating zones, yielding a non-smooth and non-convex cost surface. The **active power loss** (PL) is the total real-power loss in the transmission network, and the **emission** (E) aggregates the harmful gaseous pollutants as a mixed quadratic-and-exponential function of generation. Voltage deviation (DV) is used as an auxiliary objective in one case. These objectives are optimized two and three at a time, as summarized in Table 1.

**Table 1:** Summary of the ten multi-objective OPF case studies

Case	Test system	Objectives optimized simultaneously	$n_t$
1	IEEE 30-bus	QFC + PL	2
2	IEEE 30-bus	QFC + E	2
3	IEEE 30-bus	TFC + PL	2
4	IEEE 30-bus	TFC + E	2
5	IEEE 30-bus	QFC + PL + E	3
6	IEEE 30-bus	TFC + PL + E	3
7	IEEE 57-bus	TFC + PL	2
8	IEEE 57-bus	TFC + PL + E	3
9	IEEE 118-bus	TFC + PL + E	3
10	IEEE 118-bus	TFC + PL + DV	3

$n_t$  denotes the number of objectives optimized simultaneously (QFC: quadratic fuel cost; TFC: total fuel cost; PL: active power loss; E: emission; DV: voltage deviation)

## 3. Archive-Based MOIMO

### 3.1. The Ions Motion Optimization Algorithm

IMO is a population-based metaheuristic inspired by the attraction and repulsion forces between oppositely and like-charged ions<sup>[5]</sup>. The population is split into anions and cations, which together represent candidate solutions. Anions are drawn toward the best cation and cations toward the best anion, with the magnitude of the attraction force inversely related to the inter-ion distance. The search proceeds in two phases. In the liquid phase the ions move freely under the dominant attraction force, providing exploration; the position updates contain no random component, so the swarm steadily converges toward the best opposite-charge ion. As iterations advance and ions approach the optimum, the algorithm enters the crystal phase, in which a controlled repulsion and occasional re-initialization disperse the ions to escape local optima before the population melts back into the liquid phase. This alternation balances exploration and exploitation throughout the run.

### 3.2. Multi-objective Extension

To handle several objectives, the single-objective IMO is coupled with an external archive and a leader-selection strategy. The archive stores the best non-dominated solutions discovered during the search; at every iteration newly generated solutions are compared with the archive members, dominated members are removed, and the archive is truncated to its capacity whenever it overflows. To preserve a uniform spread, the leaders that guide the anion and cation movements are chosen from the least-crowded regions of the archive, measured by a crowding metric. This mechanism drives the search toward sparse portions of the Pareto front and improves overall coverage, while the underlying liquid-crystal dynamics retain the convergence behaviour of IMO. The resulting algorithm is referred to as MOIMO.

Constraints—including the equality power-balance equations, the inequality operating limits and the discontinuities introduced by prohibited operating zones in the total-fuel-cost formulation—are enforced through a

penalty approach rather than through stochastic repair. A solution that violates any constraint, or that falls inside a prohibited operating zone, has its fitness penalized so heavily that it is dominated by every feasible candidate and is therefore excluded from the archive. Because the archive and the leader set retain only feasible non-dominated members, the attraction vectors that drive the deterministic liquid-phase movement are always directed toward feasible leaders; the penalty thus steers the swarm around forbidden regions without requiring an explicit random jump. This keeps the search feasible while preserving the convergence behaviour of the underlying IMO dynamics.

**3.3. Decision Making and Performance Metrics**

Because the archive returns a set of equally valid solutions, a fuzzy decision-making procedure is used to extract a single best compromised solution (BCS) for the operator. Each objective of every non-dominated solution is mapped to a fuzzy membership in the range [0, 1], with a membership of one for the best value of that objective and zero for the worst; the solution whose normalized aggregate membership is highest is reported as the BCS. Algorithmic performance is assessed by the spread of the best Pareto front [12], the average computation time over thirty independent runs, the median and standard deviation of the hyper-volume (HV) indicator—which jointly captures convergence and coverage [13, 14]—and by the Friedman [15], Friedman-aligned [16] and Quade [17]

statistical tests applied to the HV values.

**4. Results and Discussion**

MOIMO was compared with six contemporary archive-based optimizers—MODA [9], MOALO [11], MOGWO [6], MOMVO [7], MOSSA [8] and MOMFO [10]—on the ten cases of Table 1. For a fair comparison the archive size, population and iteration count were fixed at 100, 250 and 500 for all algorithms, each run thirty times independently. The algorithms were implemented in MATLAB, and the power flow was solved with MATPOWER [19].

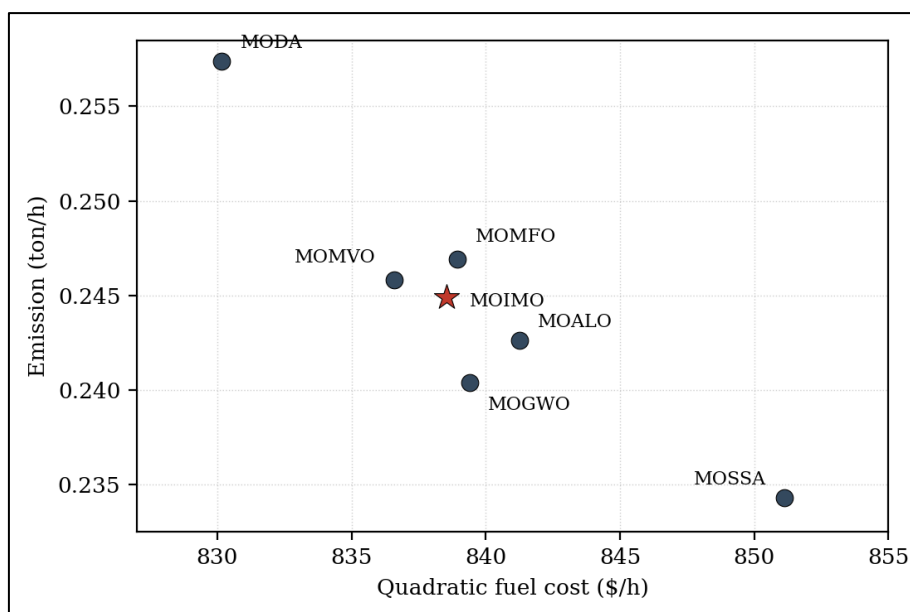
**4.1. Best Compromised Solution and Pareto Fronts**

Table 2 lists the exact BCS values for representative cases. In Case 1 (quadratic fuel cost and active power loss on the IEEE 30-bus system) MOMVO obtained the lowest fuel cost of 833.453 \$/h while MOIMO obtained the lowest loss of 4.6986 MW; no single algorithm dominated both objectives, which is the expected outcome for conflicting goals. Across the ten cases each objective minimum was captured by a different algorithm, so the methods cannot be ranked by BCS alone. The study reports that MOIMO produced comparatively uniformly distributed Pareto fronts in several cases. Figure 1 plots the BCS points obtained for Case 2 (quadratic fuel cost versus emission): the solutions are spread along a conflicting trade-off, with MOIMO occupying a balanced central position rather than an extreme.

**Table 2:** Best compromised solution (BCS) values for selected cases (exact values from the study)

Case	Objective	MOMFO	MOGWO	MOMVO	MOSSA	MOALO	MODA	MOIMO
1	QFC (\$/h)	839.72	841.73	833.45	858.49	848.28	851.59	851.15
	PL (MW)	6.0063	5.1353	5.3223	4.7882	4.7306	4.9945	4.6986
2	QFC (\$/h)	838.94	839.40	836.59	851.13	841.25	830.17	838.55
	E (ton/h)	0.2469	0.2404	0.2458	0.2343	0.2426	0.2574	0.2449
7	QFC (\$/h)	42334	41839	41784	42500	42112	43362	42210
	PL (MW)	17.35	11.95	11.27	12.43	10.51	12.04	10.26
9	TFC (\$/h)	72600	71534	70368	72035	70468	71569	70217
	PL (MW)	132.51	81.15	89.42	85.93	66.05	47.60	48.07

No single algorithm attains the best value of every objective, confirming the conflicting nature of the goals.



**Fig 1:** Best compromised solutions of the seven archive-based algorithms for Case 2 (quadratic fuel cost versus emission, IEEE 30-bus). MOIMO (star) lies in the central trade-off region; the objectives conflict, so no point dominates the others

### 4.2. Computation Time, Hyper-volume and Robustness

Average computation time over thirty runs is shown in Figure 2 for cases that trace the full scaling path—from the small 30-bus two-objective case, through the 57-bus problem at two and then three objectives, to the large 118-bus three-objective cases. Computation time rises with both system size and the number of objectives, as expected. MOIMO is consistently

among the faster methods—comparable to MOGWO and MOMVO and markedly faster than MODA and MOMFO on the larger IEEE 57- and 118-bus systems—while MODA is the slowest throughout. The hyper-volume indicator, which jointly reflects convergence, diversity and cardinality, was compared by its median value over the runs; the rankings vary case by case, with no algorithm dominating all ten.

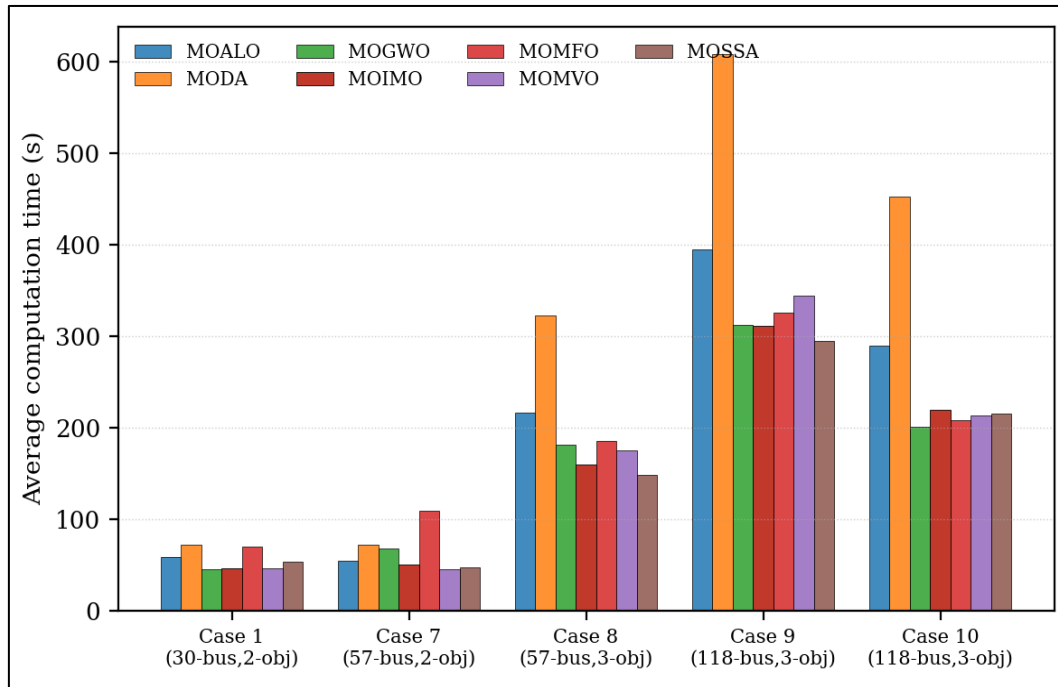


**Fig 2:** Average computation time of the seven algorithms along the scaling path (30-bus 2-objective → 57-bus 2- and 3-objective → 118-bus 3-objective). Time grows with system size and objective count; MODA is slowest while MOIMO stays competitive on the largest systems

The clearest strength of MOIMO appeared in the standard deviation of the hyper-volume, a measure of run-to-run robustness. Counting the cases in which each algorithm attained the lowest standard deviation of HV (Figure 3), MOIMO leads with four of the ten cases—more than any

competitor. A low spread of hyper-volume means the quality of the returned Pareto set is stable across independent runs, an attractive property for an operational tool that must behave predictably.

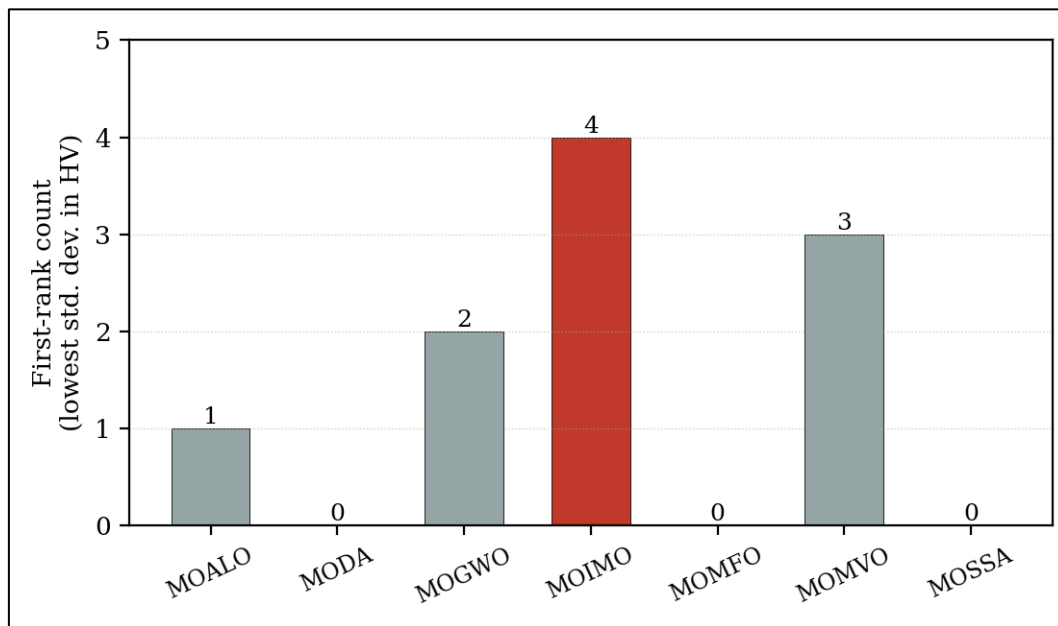


**Fig 3:** Number of cases (out of ten) in which each algorithm achieved the lowest standard deviation of hyper-volume. MOIMO is the most robust

To establish whether the differences are significant, the Friedman, Friedman-aligned and Quade tests were applied to the HV values; their rank values are shown together in Figure 4 (the Friedman and Friedman-aligned values share the left axis, while the Quade values, which lie on a smaller scale, use the right axis). All three tests agree on the overall ordering: MOMVO ranks first, followed by MOGWO, MOALO, MOSSA and MODA, with MOIMO and MOMFO last. This agreement among tests with different block-

handling mechanics lends confidence to the conclusion that no method is uniformly best—consistent with the No Free Lunch theorem [4]. MOIMO ranks in the lower half of the field on these aggregate tests, so its advantage lies specifically in Pareto-front uniformity and in robustness rather than in the aggregate statistical ranking. Taken together, the four views show that the apparent winner depends on the criterion, and that MOIMO is a strong contender whose merit is consistency.

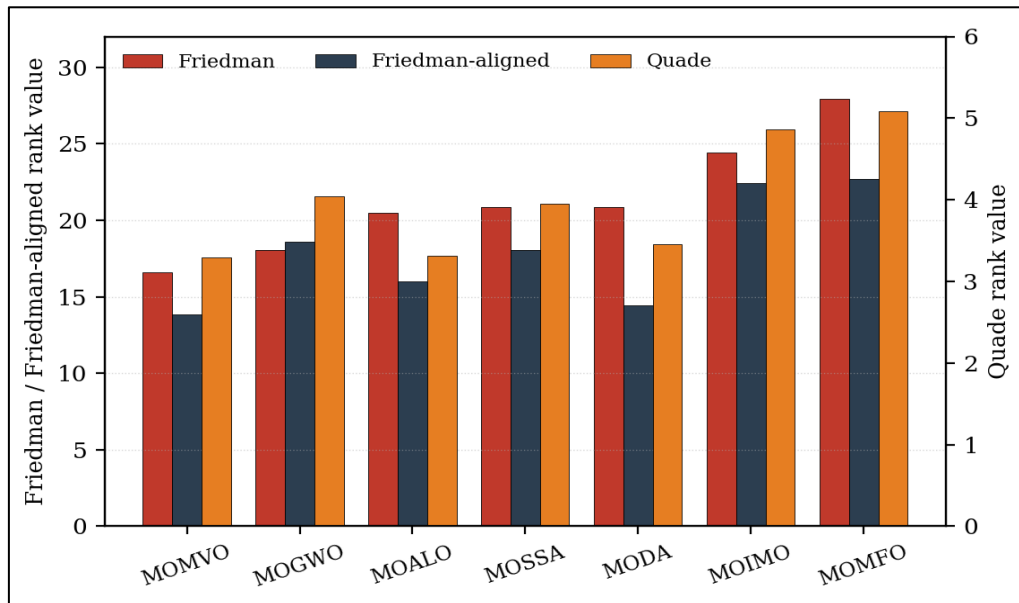


**Fig 4:** Rank values of the seven algorithms under the Friedman, Friedman-aligned and Quade tests applied to the hyper-volume results (lower is better). Quade values use the right-hand axis. All three tests rank MOMVO first and MOMFO last; MOIMO lies in the lower half

It is worth noting that a single population of 250 individuals was used for every case, from the IEEE 30-bus system to the IEEE 118-bus system whose control vector exceeds seventy dimensions. A fixed, comparatively economical population is demanding on the larger systems, where a richer Pareto front would benefit from a larger search population, and this partly explains why no algorithm—including MOIMO—dominated the aggregate statistical ranking on the high-dimensional cases. Even under this restricted and computationally economical setting, however, MOIMO retained the lowest standard deviation of hyper-volume in four of the ten cases, indicating that its run-to-run consistency is robust to the dimensionality of the problem rather than an artefact of a generous population budget.

**5. Techno-Economic-Environmental Benefit Assessment**

The practical merit of a MOOPF solution is best expressed in operational savings. The best compromised solution obtained with MOIMO for Case 2—the simultaneous optimization of quadratic fuel cost and emission on the IEEE 30-bus

system—was therefore compared against a reported method, the multi-objective firefly algorithm with constraints-prior Pareto-domination (MOFA-CPA) [18], and the per-hour improvements were annualized. MOIMO reached a compromise fuel cost of 838.551 \$/h against 852.02 \$/h for the reported method, a saving of 13.469 \$/h that, scaled over 8,760 hours, amounts to 117,988 \$ per year. Over the same solution the emission fell from 0.279 to 0.2449 ton/h, a reduction of 0.0341 ton/h or 298.716 tons per year. These quantities are summarized in Table 3 and visualized in Figure 5. The annualization assumes the system holds the Case 2 operating point at constant load for the full year; it therefore represents an upper-bound potential saving rather than a load-following operational figure, and a refined estimate would weigh the hourly saving by a load-duration curve. Even as an upper bound, the result translates the abstract Pareto improvement into tangible operational value and shows that the diversity-preserving behaviour of MOIMO yields real economic and environmental gain, not merely a numerical nicety.

**Table 3:** Annualized techno-economic-environmental benefit of MOIMO over the reported MOFA-CPA method [18] (Case 2, QFC + E)

Quantity	MOIMO	MOFA-CPA	Annual benefit
Quadratic fuel cost (\$/h)	838.551	852.02	117,988 \$/yr
Emission (ton/h)	0.2449	0.279	298.716 tons/yr

Annual benefit = (MOFA-CPA – MOIMO) per hour × 8,760 h, assuming the Case 2 operating point is held at constant load for the full year (upper-bound estimate)

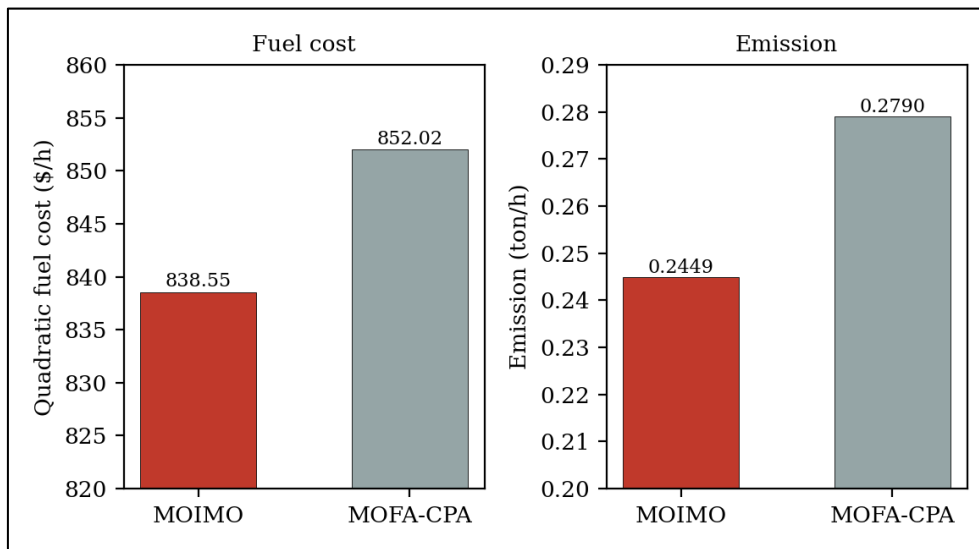


**Fig 5:** Case 2 best-compromised fuel cost and emission of MOIMO compared with the reported MOFA-CPA method. MOIMO is lower on both objectives for this compromise solution

## 6. Conclusion

This paper presented an archive-based multi-objective Ions Motion Optimization algorithm and applied it to the multi-objective optimal power flow problem. By combining the liquid-crystal search dynamics of IMO with an external archive and crowding-aware leader selection, MOIMO was evaluated against six contemporary archive-based optimizers on ten cases over the IEEE 30-, 57- and 118-bus systems. No method dominated on every objective, and statistical tests on hyper-volume ranked MOMVO first overall, consistent with the No Free Lunch theorem [4]; MOIMO's distinctive strengths were the uniformity of its Pareto fronts and its run-to-run robustness, attaining the lowest standard deviation of hyper-volume in four of the ten cases—more than any competitor. For the quadratic-fuel-cost-and-emission case, the MOIMO compromise solution yielded an annual fuel saving of 117,988 \$ and an emission reduction of 298.716 tons relative to the reported MOFA-CPA method [18]. Future work will study the exploration-exploitation balance of the underlying operators, incorporate multi-attribute decision making to select an algorithm according to operator preference, and extend the approach to OPF formulations that include FACTS devices, unit commitment and the scheduling of electric vehicles.

## 7. References

1. Buch H, Trivedi IN. On the efficiency of metaheuristics for solving the optimal power flow. *Neural Computing and Applications*. 2019;31(9):5609-27.
2. Warid W, Hizam H, Mariun N, Abdul-Wahab NI. Optimal power flow using the Jaya algorithm. *Energies*. 2016;9(9):678.
3. Zhang J, Tang Q, Li P, Deng D, Chen Y. A modified MOEA/D approach to the solution of multi-objective optimal power flow problem. *Applied Soft Computing*. 2016;47:494-514.
4. Wolpert DH, Macready WG. No free lunch theorems for optimization. *IEEE Transactions on Evolutionary Computation*. 1997;1(1):67-82.
5. Javidy B, Hatamlou A, Mirjalili S. Ions motion algorithm for solving optimization problems. *Applied Soft Computing*. 2015;32:72-9.
6. Mirjalili S, Saremi S, Mirjalili SM, Coelho L dos S. Multi-objective grey wolf optimizer: A novel algorithm for multi-criterion optimization. *Expert Systems with Applications*. 2016;47:106-19.
7. Mirjalili S, Jangir P, Mirjalili SZ, Saremi S, Trivedi IN. Optimization of problems with multiple objectives using the multi-verse optimization algorithm. *Knowledge-Based Systems*. 2017;134:50-71.
8. Mirjalili S, Gandomi AH, Mirjalili SZ, Saremi S, Faris H, Mirjalili SM. Salp swarm algorithm: A bio-inspired optimizer for engineering design problems. *Advances in Engineering Software*. 2017;114:163-91.
9. Mirjalili S. Dragonfly algorithm: A new meta-heuristic optimization technique for solving single-objective, discrete, and multi-objective problems. *Neural Computing and Applications*. 2016;27(4):1053-73.
10. Vikas, Nanda SJ. Multi-objective moth flame optimization. In: *Proceedings of the 2016 International Conference on Advances in Computing, Communications and Informatics (ICACCI)*; 2016. p. 2470-6.
11. Mirjalili S, Jangir P, Saremi S. Multi-objective ant lion optimizer: A multi-objective optimization algorithm for solving engineering problems. *Applied Intelligence*. 2017;46(1):79-95.
12. Schott JR. Fault tolerant design using single and multicriteria genetic algorithm optimization [master's thesis]. Massachusetts (MA): Massachusetts Institute of Technology; 1995.
13. Zitzler E, Thiele L. Multiobjective optimization using evolutionary algorithms — A comparative case study. In: *Parallel Problem Solving from Nature — PPSN V*. Berlin: Springer; 1998. p. 292-301.
14. Riquelme N, Von Lüken C, Barán B. Performance metrics in multi-objective optimization. In: *Proceedings of the 2015 Latin American Computing Conference (CLEI)*; 2015. p. 1-11.
15. Friedman M. The use of ranks to avoid the assumption of normality implicit in the analysis of variance. *Journal of the American Statistical Association*. 1937;32(200):675-701.
16. Friedman M. A comparison of alternative tests of significance for the problem of m rankings. *Annals of Mathematical Statistics*. 1940;11(1):86-92.

17. Quade D. Using weighted rankings in the analysis of complete blocks with additive block effects. *Journal of the American Statistical Association*. 1979;74(367):680-3.
18. Chen G, Yi X, Zhang Z, Lei H. Solving the multi-objective optimal power flow problem using the multi-objective firefly algorithm with a constraints-prior Pareto-domination approach. *Energies*. 2018;11(12):3438.
19. Zimmerman RD, Murillo-Sánchez CE, Thomas RJ. MATPOWER: Steady-state operations, planning, and analysis tools for power systems research and education. *IEEE Transactions on Power Systems*. 2011;26(1):12-19.